

**GRAIN BOUNDARY SLIDING DURING ‘DISLOCATION CREEP’ OF ICE.** T.F. Hager and D.L. Goldsby, Department of Earth and Environmental Science, University of Pennsylvania, Philadelphia, PA, 19104; [tfhager@sas.upenn.edu](mailto:tfhager@sas.upenn.edu); [dgoldsby@sas.upenn.edu](mailto:dgoldsby@sas.upenn.edu)

**Introduction:** The rheological behavior of materials is often described by a constitutive equation of the form  $\dot{\epsilon} = Ad^{-p}\sigma^n \exp\left(-\frac{Q}{RT}\right)$ , where  $\dot{\epsilon}$  is strain rate,  $A$  is a materials parameter,  $d$  is the grain size,  $p$  the grain size exponent,  $\sigma$  the stress,  $Q$  the activation energy,  $R$  the gas constant and  $T$  the temperature. Deformation experiments on polycrystalline ice reveal the existence of multiple creep mechanisms, each of which dominates for different conditions of  $d$ ,  $\sigma$  and  $T$ . At comparatively low stresses, ice deforms via a creep mechanism in which dislocation slip on the basal plane and grain boundary sliding GBS are mutually accommodating deformation processes [1-3]. This dislocation-accommodated GBS creep mechanism, characterized by values of  $n=1.8$  and  $p=1.4$ , dominates the rheological behavior of ice at sufficiently low stresses in terrestrial glaciological and planetological settings [1,3]. At higher stresses, a transition occurs to dislocation creep in ice, wherein deformation occurs via the activation of basal and non-basal dislocation slip systems. Dislocation creep of ice has been characterized by a value of  $n\sim 4$  and has been deemed to be independent of grain size, i.e., with  $p=0$  [1].

Here we demonstrate that ‘dislocation creep’ of ice exhibits a marked dependence on grain size. This grain size dependence likely indicates that GBS contributes to the creep rate of ice even in the ‘dislocation creep’ regime. A broad conclusion from this study is that deformation of ice in planetary environments, whether by diffusion creep, dislocation-accommodated GBS, or ‘dislocation creep’, is always sensitive to grain size.

**Methods:** Details of methods used to fabricate samples, deform the samples, and analyze their microstructures are given below.

*Sample preparation.* Deformation experiments were conducted on polycrystalline ice samples with well-controlled initial grain sizes. Cylindrical samples  $\sim 25.4$  mm in diameter and about 50 mm in length were fabricated via two methods. Coarser-grained samples with uniform grain sizes of 0.2 and 2 mm were fabricated by crushing ice in a blender, sieving the ice to the desired grain size, packing the sieved powders into steel molding tubes, evacuating the powders, then flooding the evacuated powders at a temperature of 273 K. The flooded samples were then frozen from below in an effort to exclude any air bubbles. The ice powders served as seeds for crystal growth in the flooded samples, which controls the grain size. Fine-grained

samples with grain sizes of  $\sim 20$   $\mu\text{m}$  were prepared by directing a mist of water from a pneumatic nebulizer into liquid nitrogen, boiling off the nitrogen, pressing the dry powders into indium jackets, sealing the powders inside the indium jackets with a soldering iron, and evacuating while densifying the samples in the high-pressure gas apparatus prior to testing.

Coarser-grained samples were cut to the appropriate size and sealed in indium jackets prior to the deformation experiments. Already-jacketed fine-grained samples were removed from the high-pressure apparatus after densification and measured, then reloaded in the apparatus for deformation. The indium jackets are a barrier to the high-pressure gas, providing confinement of the samples to prevent fracturing at the comparatively high stresses of the experiments.

*Deformation experiments.* Samples were deformed in a high-pressure gas apparatus designed for cryogenic use at nominally constant strain rate, by driving the deformation piston into the pressure vessel at a controlled displacement rate. From the resulting stress

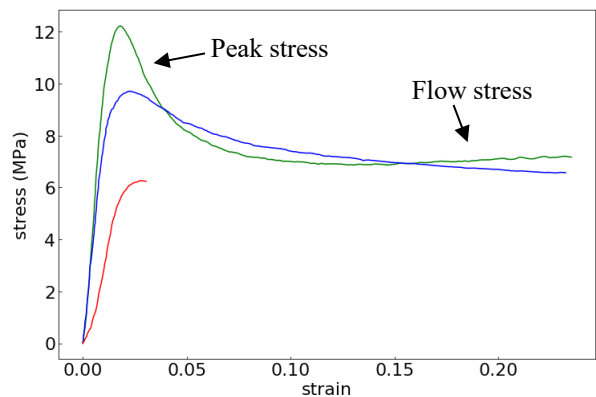


**Figure 1** – Plot showing stress-strain curves for samples with grain sizes of  $\sim 2$  mm (in green),  $\sim 0.2$  mm (in blue), and  $\sim 20$   $\mu\text{m}$  (in red).

vs. strain curves, we determined both the initial ‘peak stress’, which occurs at a strain of 2-4%, as well as the approximately steady-state ‘flow stress’, obtained at larger strains. The experiments were conducted at temperatures in the range  $243 \leq T \leq 263$  K and strain rates in the range  $10^{-5} \leq \dot{\epsilon} \leq 10^{-3}$   $\text{s}^{-1}$ . The relatively high strain rates allow exploration of the dislocation creep regime in ice, even for samples with a grain size as small as  $\sim 20$   $\mu\text{m}$ . After testing, samples were quenched in liquid nitrogen to preserve their microstructures.

*Microstructural analyses.* Sample microstructures were analyzed using electron backscatter diffraction (EBSD) methods in a FEI Quanta field emission gun, environmental scanning electron microscope in the Singh Nanotech Center at the University of Pennsylvania. EBSD data yield grain-scale maps of the crystallographic orientation of grains and thus can be used to determine grain size and shape [4].

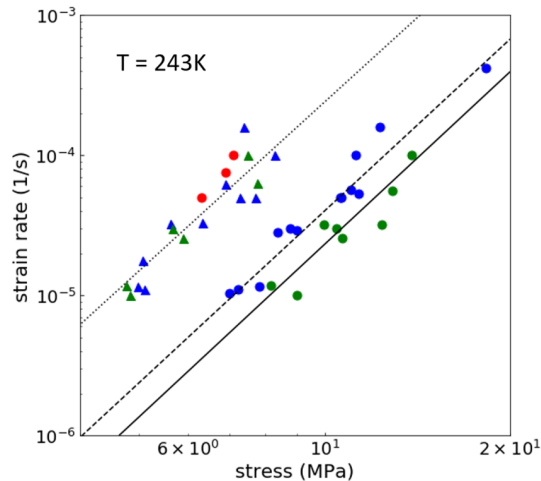


**Figure 2** – Plot of stress vs. strain rate for samples deformed at 243 K. The slopes of the data on the plot give the values of the stress exponent, with  $n \sim 4$ . The solid dots are peak-stress data for samples with grain sizes of  $\sim 2$  mm (in green),  $\sim 0.2$  mm (in blue) and  $\sim 20$   $\mu\text{m}$  (in red). The triangles are the corresponding flow-stress data for samples with grain sizes of 2 and 0.2 mm. The solid line is a fit to the green data, the dashed line a fit to the blue data, and the dotted line a fit to the aggregate flow-stress data.

**Results:** Rheological data from the experiments were analyzed using the constitutive equation given above. Figure 1 shows stress vs. strain curves from experiments on samples with grain sizes of 2 mm, 0.2 mm, and 20  $\mu\text{m}$ . As shown in the figure, the value of the peak stress increases with increasing grain size of the samples (equivalently, the strain rate of the samples increases with decreasing grain size at a given stress). With increasing strain, the curves merge together to a common flow stress.

In Figure 2, the strain rate is plotted vs. the peak stress, as well as vs. the flow stress, for each sample, on logarithmic axes, so that the slopes of the data give the values of  $n$ . As can be seen in the figure, the peak-stress data and the flow-stress data for the various samples yield a value of  $n$  of  $\sim 4$ , indicating that all of the samples are deforming via the same deformation mechanism. However, the peak-stress data show that the stress at a given strain rate increases with increasing grain size, while the flow-stress data indicate that at a given strain rate the flow stresses are approximately the same for samples of different initial grain size. A fit to the peak-

stress data yields a value of  $p$  approximately equal to 0.6. The strengthening with increasing grain size trend is opposite to the well-known Hall-Petch behavior in materials, whereby the stress at a given strain rate increases with decreasing grain size [5]. The observed increase in stress with increasing grain size for the peak-stress data is consistent with a significant contribution to the strain rate from GBS.

**Discussion and Conclusions:** The dependence of strain rate on grain size observed in the peak-stress data is consistent with a significant contribution to the strain rate from GBS in what has heretofore been described as the dislocation creep regime for ice [1]. At the peak stress, insufficient strain has accrued to alter the initial grain size due to dynamic recrystallization, and the data reveal a dependence of peak stress on grain size that is characteristic of GBS. With increasing strain, the grain size is reduced due to dynamic recrystallization. At a given strain rate, samples of different initial grain size eventually obtain the same recrystallized grain size, giving rise to nearly identical flow stresses (Figure 2).

A model that unifies the observations in both the dislocation-accommodated GBS creep regime and the ‘dislocation creep’ regime observed here is that due to Langdon [6]. In the Langdon model, GBS is impeded by the pileup of dislocations at either subgrain boundaries within a material, or at grain boundaries, with the rate of GBS determined by the climb of dislocations in subgrain boundaries or grain boundaries. The model predicts two behaviors, depending on the grain size. In the small grain size limit, when the grain size is smaller than the subgrain size (i.e., when there are no subgrains), GBS is impeded by dislocation pile ups at grain boundaries. In this case, the model predicts that  $\dot{\epsilon} \propto \frac{\sigma^2}{d^2}$ , in fair to good agreement with values of  $n=1.8$  and  $p=1.4$  in the dislocation-accommodated GBS creep regime. In the larger grain size limit, when the grain size is larger than the subgrain size (i.e., when subgrains exist), the model predicts a higher stress exponent,  $n=3$ , and a diminished grain size dependence, with  $p=1$ . Our data (with  $n=3.6$  and  $p=0.6$ ) are in fair to good agreement with that prediction.

A consequence of our study is that the flow of ice in natural settings, no matter the operative creep mechanism, will *always* be sensitive to grain size.

**References:** [1] Goldsby, D.L. and Kohlstedt, D.L. (2001) *JGR*, 106, 11017-11030. [2] Goldsby, D.L. and Kohlstedt, D.L. (1997) *Scripta Mat.*, 37, 1399-1406. [3] Durham, W.B. et al. (2010) *Space Sci. Rev.*, 153, 273-298, doi:10.1007/s11214-009-9619-1. [4] Prior, D.L. et al. (2015) *J. Microscopy*, 259, 237-256. [5] Li, Y. et al. (2016) *Proc. Roy. Soc. A*, 472, 20150890. [6] Langdon, T.G. (1994) *Acta Met.*, 42, 2437-2443.